Axial organization of muscular myosin identified by the optical and computational pipeline FAMOUS

Claire Lefort, Mathieu Chalvidal, Fabienne Baraige, Alexis Parente, Erwan Ferrandon, Véronique Blanquet, Henri Massias, Laetitia Magnol, Emilie Chouzenoux

Axial organization of muscular myosin identified by the optical and computational pipeline FAMOUS

C. Lefort*[a], M. Chalvidal[b], F. Baraige[c], A. Parenté[c], E. Ferrandon[a], V. Blanquet[c], H. Massias[a], L. Magnol[c] and E. Chouzenoux[d],
[a] CNRS UMR 7252, XLIM Research Institute, Université de Limoges, France
[b] CerCo, UMR CNRS 5549, Université Paul Sabatier, Toulouse, France
[c] PEIRENE, EA7500, USC 1061 INRAE, Université de Limoges, Limoges, France
[d] Center for Visual Computing, CentraleSupélec, Inria Saclay, Université Paris-Saclay, France

ABSTRACT

In a medical use, ultrastructure of muscle is currently revealed by images of resected samples achieved thanks to Electron Microscopy (EM), requiring freezing and paraffin sections, with a set of histological, molecular and biochemical analyses. The resection, slicing and labelling steps cause an alteration of the phenotypic and volumetric information compared to their initial integrity. Starting from this statement, we have developed an original pipeline resting on the imbrication of an optical and computational strategy for imaging 3D biomedical structures without resorting to slicing, freezing and labelling steps. The assembly of myosin of a whole muscle is revealed thanks to the second harmonic generation (SHG) recorded with a multiphoton microscope, all along the entire 180 µm of thickness of the Extensor digitorum longus (EDL) of a wild mouse. During the SHG recording, the Point-Spread-Function (PSF) of the multiphoton microscope is recorded all along the imaging depth. This step highlights an axial broadening of the PSF while maintaining a constant planar PSF throughout the whole depth of the recordings. Then, a fitting algorithm estimated a mathematical model of the PSF, highlighting its variability into the whole image depth. Finally, a computational image restauration is led thanks to the fast image deblurring algorithm BD3MG accounting for the depth variant PSF. The non-stationary distortions all along the recorded image is employed thus correcting accurately the image distortion. The axial organization of the myosin is revealed for the first time, highlighting tubular organization of myosin into the myofibrils.

Keywords: Multiphoton microscopy, computational estimation of the PSF, myosin muscle structure

1. INTRODUCTION

The typical diagnosis of muscular pathologies rests on a set of histological arguments (freezing and paraffin sections), combined with electron microscopy (EM) and molecular or biochemical analyzes. Genetic analysis has highlighted that many genes can be at the origin of some of these diseases. Reversely, a gene can be associated to several phenotypes and the same pathological phenotype can result from several genetic alterations. Histological data, EM, genetic and molecular biology do not necessarily allow a good understanding of the pathophysiology of the disease and of the precise ultrastructural abnormalities that lead to the clinical pictures [1]. The distinction among these pathologies from all dystrophic diseases and the relevance of the diagnosis of muscular defects can be improved thanks to the implementation of a new instrumental strategy. Thus, the simultaneous and label-free colocalization of structures and molecules need to be accessible at the microscopic scale while generating 3D images. A new technological and instrumental challenge is thus opened.

Multiphoton microscopy (MPM) is a dynamic, multimodal and label-free optical solution, delivering 3D images at unequaled imaging depths and sometimes without the necessity of an exogeneous labelling process [2]. This optical solution of microscopy has been demonstrated for muscle imaging thus revealing its ultrastructure [3, 4]. The emission of signals resulting from multiphoton probing processes depends on excitation light parameters and biological sensors [5]. Two nonlinear probing processes are usually involved in MPM; two-photon fluorescence and second harmonic generation. These two processes can coexist for a single sample considering the presence of fluorophores (endogenous or exogeneous) and a biological constituent structured in a noncentrosymmetric assembly, thus able to produce a second

harmonic signal. Myosin is a muscular probe of interest for revealing muscle organization [4, 6, 7]. Its noncentrosymmetric assembly gives to this protein a nonlinear optical property, here fathomable thanks to second harmonic generation (SHG), thus revealing its organization at submicronic scale. Myosin is constituting a network contained into the A bands of the sarcomere whose dimensions are between 1.9 µm until 2.5 µm [8]. But optical microscopy faces to a limitation in resolution performance. Indeed, the resolution in the optical plan (perpendicular to the optical axis) of about 250 nm at best and the resolution in the optical axis is about 1.5 µm at best. But we have recently demonstrated that in a biological sample constituted by many scattering or absorbing elements, or in case of specific laser excitation properties, this optimal of resolution decreases quickly [9], towards 0.4 µm in the optical plane and 2.3 µm in the optical axis.

For addressing this challenge, we have developed a new instrumental and computational pipeline named FAMOUS for fast algorithm for three-dimensional (3D) multiphoton microscopy of biomedical structures, here devoted to the microscopic screening of myosin of muscle. This pipeline of deep-3D-MPM (D-3D-MPM) combines the technological solution of D-3D-MPM already mastered for biomedical imaging, with a new numerical solution resting on the estimation of the true Point-Spread-Function (PSF) of the instrument and has been described in details in [10]. Thus, these works are in line with a technological dynamic for delivering the highest image quality thanks to image restoration, considering computational technologies as important as optical technologies. In the present proceeding, we present the technical, numerical and mathematical key-points of the pipeline FAMOUS and illustrate its performance on new 3D images of the myosin assembly contained into a whole mouse muscle, unsliced and label-free.

2. INSTRUMENTAL AND COMPUTATIONAL PIPELINE FAMOUS

2.1 Structure of the instrumental and computational pipeline FAMOUS

Figure 1 summarizes the structure of the instrumental and computational pipeline FAMOUS. The standard multiphoton microscope solution is presented in the left side of Figure 1 and the computational strategy lies in the right side.

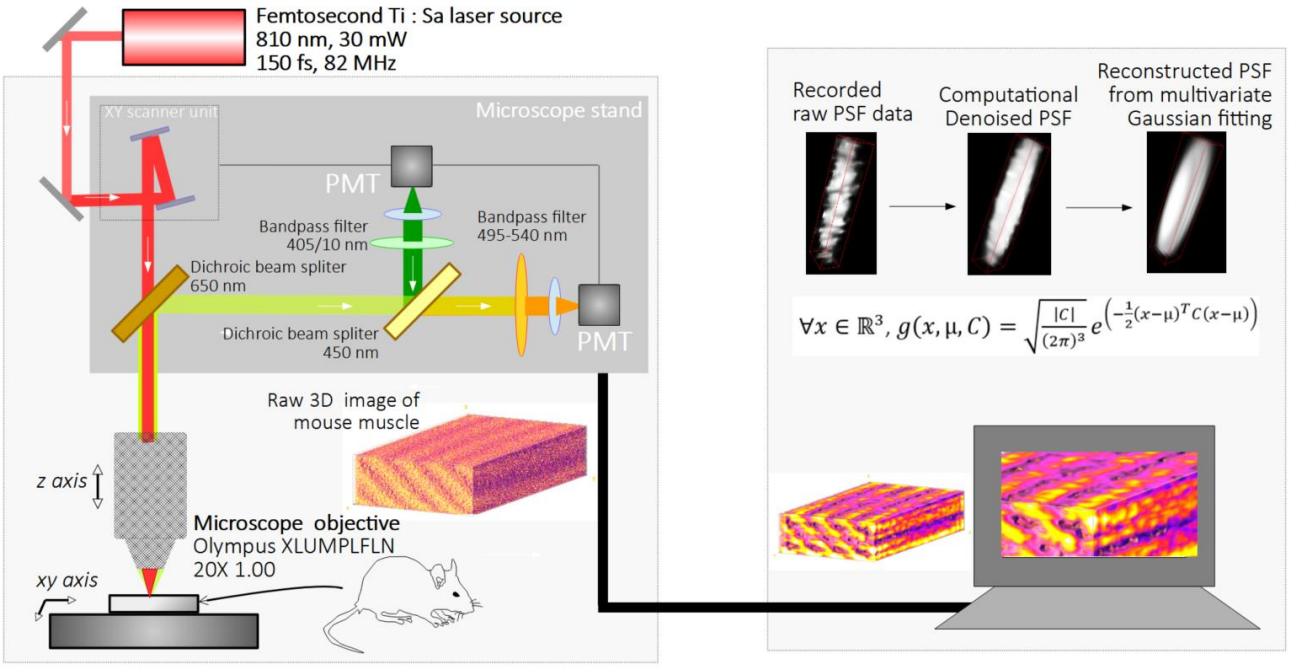

Figure 1. Structure of the instrumental and computational pipeline FAMOUS resting on a standard solution of D-3D-MPM combined with an original computational and mathematical strategy for image restauration.

The experimental setup involves a commercial multiphoton microscope BX61WI from Olympus. The excitation strategy is a tunable titanium-doped sapphire laser excitation (Ti: Sa) laser system Chameleon Ultra II, from Coherent Inc. Femtosecond pulses are delivered with a repetition rate of 82 MHz. 4 W of average power are available at the laser output. A system of average power management allows to reduce the excitation power onto the sample from 4W to 0W thanks to a half-wave-plate combined with a polarizing cube. Thus, the horizontal polarization of the laser excitation is preserved. This technical point is important considering the nonlinear excitation probing process of myosin resting on SHG depending on the relative combination between the orientation of the myofibers and the polarization of the excitation beam. The central wavelength of excitation was fixed at 810 nm. The detection of the SHG signal was led thanks to a set of dichroic mirrors, associated with bandpass filters. The water immersion objective from Olympus (XLPLN25XWMP, 25×, NA 1.05) is corrected for multiphoton acquisitions thus reducing the chromatic aberrations. A 2D scanning device allows a scanning of the sample by the excitation source. This system is composed by a galvanometric device including two mirrors. Thus, the production of 2D images of single optical plan is accessible with an adjustable scanning speed depending on the level of signal produced from the sample. In our situation, the pixel dwell time was fixed at 2 µs/pix for an image dimension of 2048 pixels × 2048 pixels. Moreover, an axial movement of the microscope objective allowed the image to be produced from different image plan into the depth of the sample. A sequential recording of 2D stacks of images all along the sample depth is produced. For the current image presented here, each image is spaced 0.1 µm apart.

2.2 Mathematical and computational strategy for D-3D-MPM image restoration

The idea of a computational solution in microscopy imaging is to restore volumetric images and to remove selectively at best the information from the image that degrades its final quality (noise, blur…) due to a combination of optical aberrations and wavefront distortions. Here, we consider the problem as a mathematical inverse problem, not considering explicitly its physical origin. In this study, muscle images are recorded thanks to a multiphoton process involving a SHG signal with an optical sectioning occurring all along the entire depth of the sample from the upper side to the bottom. Our inverse problem model assumes that the raw images produced by the microscope instrument contains both the "true" signal produced by the sample and the contribution of the instrument taking the form of a blur degradation. In a nutshell, the raw image can be seen as a convolution between the true signal emitted by the sample and the instrumental contribution, plus some noise.

The blur degradation of the image arises from wavefront distortions and optical aberrations. We consider such a combination as a whole phenomenon without explicit distinction between the origin of the distortions. The blur phenomenon is modelled numerically by a 3D convolution with a space-variant Point-Spread-Function (PSF). The latter being unknown, we rest on an experimental estimation of it recorded simultaneously with the raw signal from the myosin of muscle and all along the sample depth. The 3D PSF is not stationary in the whole 3D image (i.e., it is space-variant). We propose to record local 3D PSFs through the imaging of fluorescent microspheres with dimensions smaller than the resolution, saved simultaneously with the signal emitted from the sample (SHG). Each experimental PSF is then mathematically modeled with a 3D multivariate Gaussian fitting strategy FIGARO [11]. This allows us, in particular, to quantify and model the evolution of the PSF all along the sample depth. In a second phase of the computational part of the pipeline, the image restoration is processed thanks to a non-blind formulation of the resulting inverse problem. A penalized least-squares function is minimized, using a distributed majorize-minimize algorithm (ADD REF) accounting for our modeled variation of the PSF with depth (the axial variations of the PSF are neglected).

2.3 Mouse muscle

The muscles were selected from a 3-month-old wild-type mouse from FVB background. The extensor digitorum longus (EDL) muscles were isolated in their whole state from tendon to tendon, without lateral or longitudinal slicing processes. The integrity of the muscle was thus precisely monitored. A fixation protocol with paraformaldehyde (PFA) 4% during 12 hours at 4°C is followed by a washing procedure in phosphate-buffered saline (PBS). The microspheres were then included into the muscles thanks to a nonionic detergent, incubated 3 hours. Microspheres were composed by polystyrene beads yellow-green fluorescent and having a 0.2 µm diameter (Molecular Probes™, FluoSpheres™, yellow-green fluorescent, 0.2 µm, 505/515).

3. 3D IMAGES OF MOUSE MUSCLE PRODUCED WITH THE PIPELINE FAMOUS

Figure 2 illustrates the representation of the 3D structure of mouse muscle recorded through a D-3D-MPM. Figure 2A presents the 3D raw acquisition representating the SHG signal as recorded with the PMTs. Figure 2B represents the image resulting from the whole instrumental and computational strategy FAMOUS (Figure 1) devoted to image restoration.

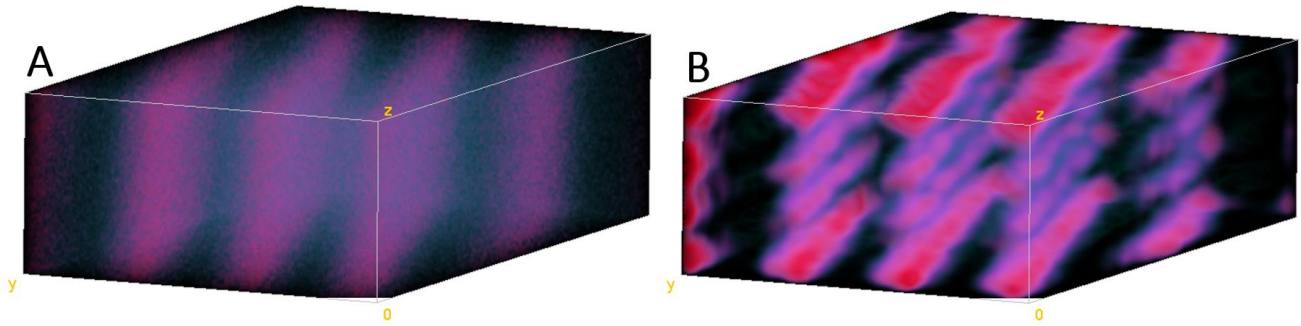

Figure 2. 3D images of mouse muscle produced with the pipeline FAMOUS. Box dimensions in the xyz directions: 14 µm × 8 µm × 6 µm. The signal recorded is the SHG from myosin of mouse muscle. A. 3D Raw image. B. Reconstructed image thank to the computational method.

For the raw 3D image (Figure 2A), the signal contained into the optical plans (XY) regardless of the recording depth delivers a coarse information. Continuous bright bands indicate the localization of the myosin assembly. By consequence, such an image can deliver an information about the width of the sarcomere, defined by the distance between two consecution dark bands. Concerning the axial plan, continuous bright bands can be observed to such an extent that the 2D observation of the horizontal plane XY could be easily mistaken for the 2D observation of the vertical plane YZ.

Concerning the restored image (Figure 2B), two new information are revealed compared to the raw images. The most evident one concerns the axial organization of myosin. From a continuous organization of the signal contained into the (YZ) plan (Figure 2A), the restored image highlights a periodical organization of the myosin thus revealing a tubular assembly of myosin. Such an organization has never been shown until now due to the absence of 3D imaging solution with a sub-micrometer resolution with a large field of view of several tens of micrometer in the three directions. The second detail revealed into the myosin assembly concerns its planar organization composed by a succession of sarcomeres. The relative position of sarcomeres is not as linear as illustrated in the raw acquisition (Figure 2A). A periodic organization seems to appear into the tubular organization of myosin. Such a detail in the optical plan looks less evident than the axial cleaning of the image. A more detailed study needs to be led before delivering new information about this organization.

4. 2D PROJECTIONS EXTRACTED FROM THE 3D IMAGE

The 3D image presented into Figure 2B highlights new information initially lost in the blur and noise of the raw image, here revealed thanks to the imaging of a whole muscle structure with a D-3D-MPM device, involving the pipeline FAMOUS. In order to better understand the axial novelty revealed thanks to this method, we are now presenting the images with a 2D representation. Figure 3 gathers the 2D representation of the 3D presented into Figure 2B, in projection all along the three axis: XY, XZ and YZ. Figure 4 proposes a superimposition of the raw and reconstructed images along the axis where new information are revealed: XZ and YZ.

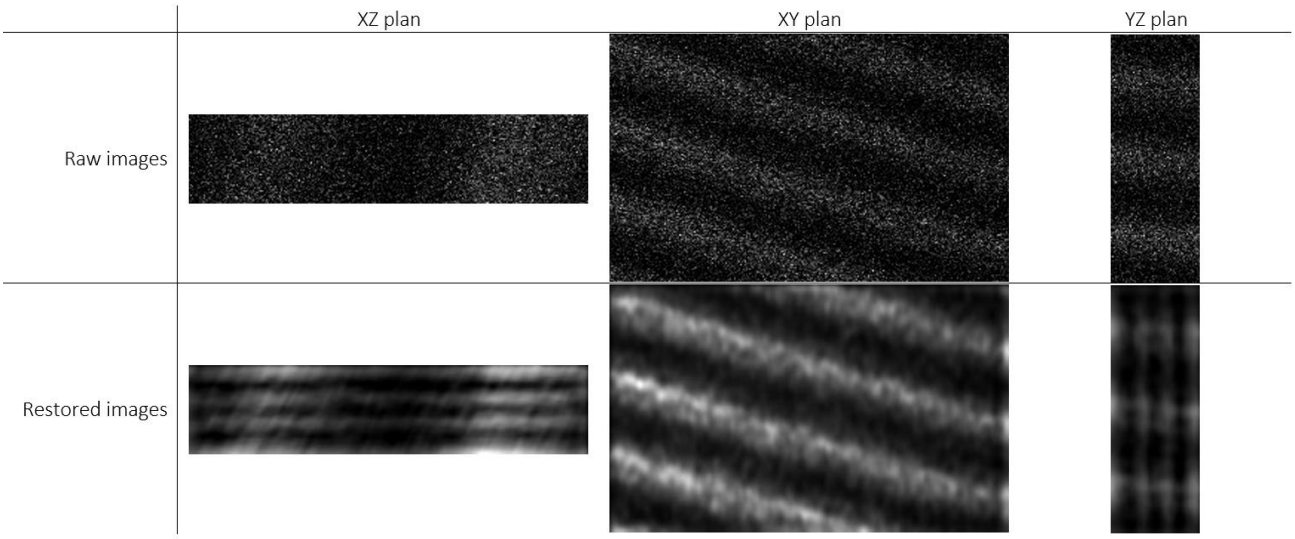

Figure 3. 2D projections of the 3D image. The raw and restored images are presented all along the 3 axis: XY, XZ and YZ. The axial organization of the myosin of muscle reveals a new organization, yet never highlighted.

Figure 4 highlights a superimposition of the raw image in red with its restored representation in green. This representation delivers a better visualization of the improvement induced on the visual quality of the image, allowing to see new details in the image.

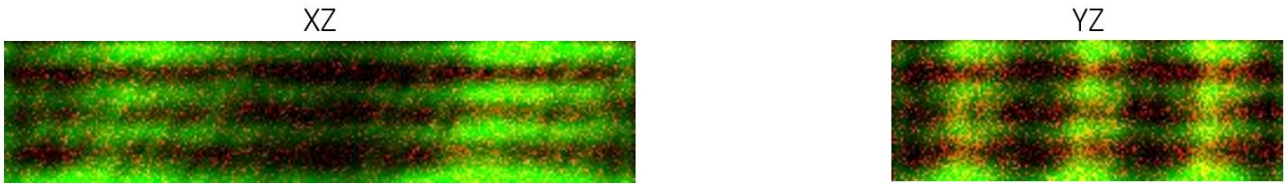

Figure 4. axial representation of raw signal (red) and reconstructed image (green) of the SHG signal emitted from the myosin assembly of muscle.

Figure 5 illustrates an analysis of the axial intensity of the emission signal before and after the image restoration process. The intensities are recorded at the same place for the raw and the restored images.

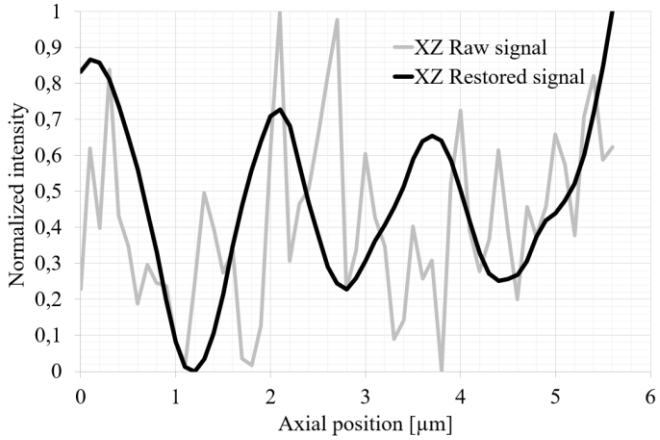

Figure 5. Analysis of the emitted raw and restored signals of SHG. The intensities are recorded at the same place between the raw and restored images. The background signal is translated to zero and the intensities are normalized.

5. DISCUSSION AND CONCLUSION

The two axial representations XZ and YZ of SHG produced by myosin assembly are revealing a new layer of information about the myosin assembly of muscle. Indeed, Figure 2, 3, 4 and 5 are showing the presence of myosin contained into discrete areas along the optical axis Z. Such a new information has never been revealed before, and for the first time we are revealing this new information thanks to our 3D imaging instrumental and computational pipeline FAMOUS, devoted to the image of a whole muscle. Considering the muscle assembly, such a view point is not yet well-known and the origin of this discretization of the signal coming from the myosin can be discussed. Indeed, the sarcomere is the basic unit of the muscle. The sarcomere is mainly constituted by an alternating of myosin and actin, two proteins whose relative movement is responsible for muscle contraction. The current representations of sarcomere are proposed thanks to electron microscopy, delivering a 2D representation of the internal constitution of the sarcomere and their relative imbrications. But the experimental representation of the 3D ultrastructure of sarcomere has never been presented. Only assumptions about the internal arrangement of the sarcomere can be given in 3D on the basis of evidence clusters. In the present work, we highlight for the first time a representation of the 3D sarcomere as a superimposition of contractile unit in the optical plan as expected, but also along the optical axis of the recorded image.

REFERENCES

[1] S. Mathis, M. Tazir, L. Magy, F. Duval, G.l Le Masson, M. Duchesne, P. Couratier, K. Ghorab, G. Solé, I. Lacoste, C. Goizet, J.-M. Vallat, “History and current difficulties in classifying inherited myopathies and muscular dystrophies”, J Neurol Sci., 384, 50-54 (2018)

[2] E. E. Hoover, J. A. Squier, “Advances in multiphoton microscopy technology”, Nature Photonics, 7, 93-101 (2013)

[3] J. Lau, C. C. Goh, S. Devi, J. Keeble, P. See, F. Ginhoux, L. G. Ng, “Intravital multiphoton imaging of mouse tibialis anterior muscle”, Intravital. 5 (2), e1156272 (2016)

[4] Q. Sun, Y. Li, S. He, C. Situ, Z. Wu, J. Y. Qu, “Label-free multimodal nonlinear optical microscopy reveals fundamental insights of skeletal muscle development”, Biomedical Optics Express, 5 (1), 158-166 (2014)

[5] T. Vo-Dinh, “Biomedica Photonics Handbook”, CRC Press, Boca Raton (2003)

[6] H. Hajjar, H. Boukhaddaoui, A. Rizgui, C. Sar, J. Berthelot, C. Perrin-Tricaud, H. Rigneault, N. Tricaud, “Label-free non-linear microscopy to measure myelin outcome in a rodent model of Charcot-Marie-Tooth diseases”, Journal of BioPhotonics, (2018)

[7] L. Moon, D. W. Frederick, J. A. Baur, L. Z. Li, “Imaging Redox State in Mouse Muscles of Different Ages”, Adv Exp Med Biol., 977, 51–57 (2017)

[8] B. M. Millman, “The filament lattice of striated muscle”, Physiol. Rev. 78 359–91 (1998)

[9] T. Hortholary, C. Carrion, E. Chouzenoux, J.-C. Pesquet, C. Lefort, “Multiplex-multiphoton microscopy and computational strategy for biomedical imaging”, Microscopy Research and Technics, 84 (7), 1553-1562 (2021)

[10] K. W. Eliceiri, M. R. Berthold, I. G Goldberg, L. Ibáñez, B. S. Manjunath, M. E Martone, R. F Murphy, H. Peng, A. L Plant, B. Roysam, N. Stuurman, J. R Swedlow, P. Tomancak, A. E Carpenter, “Biological imaging software tools”, Nature Methods, 9 (7), 697-710 (2012)

[11] E. Chouzenoux, T. T.-K. Lau, C. Lefort, J.-C. Pesquet, “Optimal Multivariate Gaussian Fitting with Applications to PSF Modeling in Two-Photon Microscopy Imaging”, 61 (7), 1037-1050 (2019)